Batteries & Supercaps

Research Article
doi.org/10.1002/batt.202300458

Chemistry Europe
European Chemical Societies Publishing

www.batteries-supercaps.org

Water-based Supercapacitors with Amino Acid Electrolytes: A Green Perspective for Capacitance Enhancement

Alessio D'Alessandro,*[a] Sebastiano Bellani,*[b] Agnese Gamberini,[b] Valentina Mastronardi,[b] Marilena Isabella Zappia,[b] Matteo Abruzzese,[b] Sanjay Thorat,[b] Elena Calcagno,[b] and Francesco Bonaccorso*[b, c]

State-of-the art Electrochemical Double-Layer Capacitors (EDLCs) usually extend their operating electrochemical stability window (ESW) by means of organic electrolytes, or highly concentrated aqueous (water-in-salt) electrolytes hindering parasitic water splitting reactions. Unfortunately, organic solvents and high concentrations of ions penalize the dielectric constant of the electrolyte, hence the capacitive performance. We suggest here a new concept of cost-effective and sustainable aqueous electrolytes based on concentrated amino acid water solutions with a dielectric permittivity much higher than pure water, unlocking the capacitive performance of aqueous EDLC references. Amino acids are natural zwitterionic molecules with a large separation between the positive and negative moiety, leading to huge dipoles with excellent dielectric properties. Some of them (*e.g.*, lysine and proline), have a solubility $\geq$10 m at ambient temperature. With an experimental characterization we prove that aqueous EDLCs based on electrolytes obtained with L- lysine or L-proline added to 2 M $NaNO_3$ solution have +50% of gravimetric capacitance enhancement at low specific currents (0.1 A/g) compared to a reference device based on 2 M $NaNO_3$ electrolyte without amino acids. A theoretical model suggests that this performance may be further enhanced by increasing the ionic accessibility of commercially available active materials, with porosity optimized to the size of amino acid ions.

Introduction

Electrochemical Double-Layer Capacitors (EDLCs) with a high energy density are usually obtained with electrodes based on nanostructured/porous carbons with high-specific surface area, *e.g.*, activated carbon, graphene, carbon nanotubes, carbide-derived nanocarbons.[1] Importantly, EDLC electrolytes must also ensure a wide electrochemical stability window (ESW) to exhibit purely capacitive behavior at high operating voltages,[2,3,4] being the energy density proportional to square of the applied voltage. Extended ESWs are typically achieved with organic electrolytes, or highly concentrated aqueous (*e.g.*, salt-in-water) electrolytes,[5,6] which hamper parasitic water electrolysis reactions. Despite organic electrolytes are commonly established in commercially available EDLCs, their aprotic polar solvents (*e.g.*, acetonitrile) are moderately toxic and flammable materials.[7,8] Also, their polarity is lower than water (dielectric constant ε_r = 36 for acetonitrile, ε_r = 64 for propylene carbonate, while ε_r = 78 for water[9,10]), with a negative impact on the $\varepsilon_r$and, in turn, on the capacitive performance of traditional EDLCs.[11] Furthermore, salts used with such solvents like quaternary ammonium tetrafluoroborates ($TEABF_4$) are also toxic[12,13] and expensive.[14] To enhance the ESW of traditional EDLCs, ionic liquid-based electrolytes (*e.g.*, EMI-TFSI, EMI-BF_4 and BMI-PF_6) and deep eutectic solvent-based electrolytes have been reported as effective options, even though their cost and/or toxicity still challenge their practical implementation.[5,6,15] The use of a highly concentrated aqueous electrolyte (*e.g.*, salt-in-water) reduces the number of free water molecules, lowering the water activity and, thus, increasing the potential of the oxygen evolution reaction (OER).[16] Despite this strategy increases the ESW of EDLCs, water dipoles already engaged in the hydration shell of the ions are less reactive to the external electric field, resulting in aqueous electrolytes with low ε_r.

To design aqueous electrolytes with wide ESW and high ε_r, highly soluble and polar additives can be used to provide the dielectric properties in the place of water. Consequently, the water content of the electrolyte can be safely reduced with no loss of ε_r while hindering water splitting reactions and excessive viscosity, which, in turn, may negatively affect the ionic conductivity. Such additives are molecules with large permanent dipoles and excellent solubility, but also thermochemical and electrochemical stability to avoid the electrolyte degradation in advanced high-voltage EDLCs.[3] Also, the size of these

[a] *Dr. A. D'Alessandro*
Ansaldo Green Tech S.p.A.
Via N. Lorenzi 8, 16152 Genova
E-mail: alessio.dalessandro@ansaldoenergia.com

[b] *Dr. S. Bellani, A. Gamberini, Dr. V. Mastronardi, Dr. M. I. Zappia, M. Abruzzese, Dr. S. Thorat, E. Calcagno, Dr. F. Bonaccorso*
BeDimensional S.p.A.
Via Lungotorrente Secca, 30R, 16163 Genova
E-mail: s.bellani@bedimensional.it
f.bonaccorso@bedimensional.it

[c] *Dr. F. Bonaccorso*
Istituto Italiano di Tecnologia
Via Morego 30, 16163 Genova

Supporting information for this article is available on the WWW under https://doi.org/10.1002/batt.202300458

Research Article
doi.org/10.1002/batt.202300458
Chemistry Europe
European Chemical Societies Publishing

polar molecules should be as small as possible to match the dimensions of the smallest electrode pores, so that they can effectively participate to the electric double layer formation.

Amino acids in their natural, zwitterionic form possess a positive and negative net charge in the same molecule, separated at a distance much larger than the OH bond in water, thus a dipole moment much larger than pure water (Figure 1), up to values of 7.34 D for (not hydrated) L-arginine. [17]

Such molecules are not only a cheap and green choice of electrolyte, but also biologically selected to withstand oxidation and extreme temperatures, and to cope with highly salted solutions. Osmolytes of amino acids and amino acid derivatives (*e.g.*, betaine and ectoine) are involved in cellular mechanisms to restore the ε_r and Debye length in extremely salted environments, thus preserving proteins against denaturation by salts.[19,20] Hydrated amino acids are also an alternative way to salts to achieve osmotic equilibrium in cells. [21,22] In this way the dielectric properties of the solution can be preserved to ensure correct protein folding, a target which would not be met with concentrated ionic osmolytes with no amino acids. Like living cells, an EDLC electrolyte must feature a high $\varepsilon_r$of the solvent in presence of salts while retaining hydration ability. For an aqueous electrolyte, water molecules engaged in the hydration shells of the zwitterionic amino acids are less available for parasitic electrolysis reactions. Lastly, concentrated L-lysine amino acid solutions are also used as anti-icing agents to investigate biologic samples and proteins at cold temperatures, [23] retaining their dielectric properties down to −40 °C. Based on these considerations, the proposed amino acid-based aqueous solutions can represent effective bio-mimicking electrolytes for advanced all-climate aqueous EDLCs.

To experimentally prove the above rationale for the design of advanced aqueous electrolytes, we selected zwitterionic L-lysine and L-proline as prototypical amino acids. In fact, these molecules have excellent water solubility (up to 1:5 molar ratio[24,25]) even in presence of additional salts, with a documented salting-in effect up to 3 M. [26] As electrolyte, we first investigated an aqueous solution of 10 m of L-proline + 2 M $NaNO_3$, which was compared with a 2 M $NaNO_3$ water solution as reference nearly pH-neutral aqueous electrolyte.[5] As a second option, we tested zwitterionic L-lysine at 10 m concentration in water without additional salts. L-lysine is a peculiar case among the 20 proteogenic amino acids because at its isoelectric point (pH ≈9.7) a relevant fraction of molecules is ionized (12% Lys^+ and 12% Lys^-) and only 76% of the species are in the zwitterionic neutral form. A unique solute, L-lysine, provides at the same time the dielectric properties (zwitterionic species) and the ionic conductivity (ionized species), offering the opportunity to study an electrolyte with no extra salts. In depth electrochemical characterization was carried out on aqueous EDCLs based on this electrolytes and electrodes made of graphene:activated carbon active materials.[5,27]

A theoretical model is then proposed to interpret the electrochemical results, providing insight on the design of novel types of high-ε_r aqueous electrolytes.

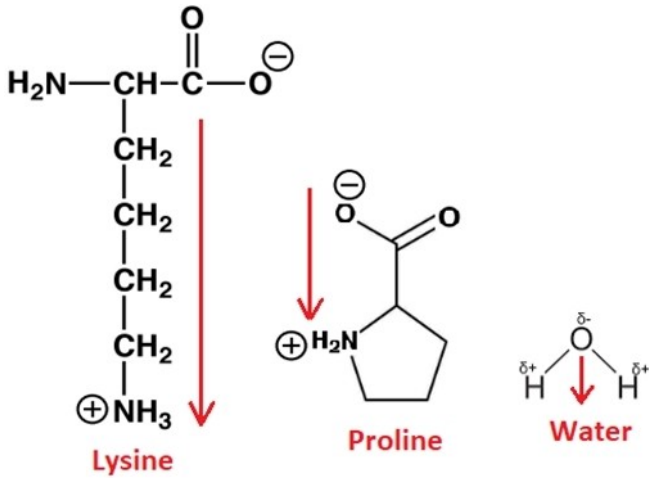

Figure 1. Water-soluble amino acids in their zwitterionic form feature a dipolar moment (red arrow) significantly larger than the one of water molecule, resulting in excellent candidates for the design of aqueous electrolytes with large dielectric permittivity. Calculated permanent dipole moments for isolated molecules (excluding hydration effects) are in the range[17] of 5.82–6.42 D for L-lysine, 5.54-6.10 D for L-proline and only 1.85 D for water.[18]

Results and Discussion

Methods

Electrolyte characterization. Three different aqueous electrolytes were studied: 1) 2 M $NaNO_3$ in water (reference electrolyte), 2) 10 m of L-proline (Pro) + 2 M $NaNO_3$ in water, 3) 10 m L-lysine (Lys) in water. The ion conductivity of the investigated aqueous electrolytes was measured using a four-point-calibrated FiveEasy FE30 conductivity meter (Mettler Toledo) at room temperature (22 °C), 40 °C, 50 °C, 60 °C and 80 °C, covering a temperature range compatible with common aqueous electrolytes. The rotational rheology of the electrolytes was measured with a Hybrid HR2 rheometer (TA instruments). More in detail, a double-wall concentric cylinder geometry was installed on the rheometer to evaluate the electrolyte viscosity in the 25–75 °C temperature range (10 °C/min ramp) at 100/s shear rate. Thermogravimetric analysis (TGA) and differential scan calorimetry (DSC) measurements were performed on the amino acids and corresponding electrolytes, respectively, using a TGA Q500 (TA Instruments, USA) thermogravimetric analyzer and applying a N_2 flow rate of 10 mL/min) and a heating rate of 10°C/min.

Electrodes fabrication. Commercial activated carbon (AB-520, MTI Corp.), few-layer graphene (BeDimensional S.p.A.), produced by wet-jet milling exfoliation of graphite, [28,29, 30] carbon black (>99.9%, Alfa Aesar), and Poly(vinyl alcohol) (PVA) (MW 89,000-98,000, 99+%, hydrolysed, Sigma Aldrich), were mixed with a 80:5:5:10 weight ratio in ultrapure water (1:4 solid/liquid weight content ratio) using a planetary centrifugal mixer, until obtaining a homogenized slurry.[31,32] The as-produced slurry was subsequently deposited on graphite paper (Papyex Flexible Graphite, Mersen) by doctor blading using a MSK-AFA–H200 A coater (MTI Corp.). The obtained electrodes were dried at 70 °C in a vacuum oven (Binder, VD 53-UL) overnight to

Research Article
doi.org/10.1002/batt.202300458
Chemistry Europe
European Chemical Societies Publishing

remove water residues. The mass loading of the electrode materials was ~2 mg/cm^2.

Cells fabrication. The EDLCs were fabricated by stacking two electrodes in a Swagelok-type cell based on 316 L stainless steel pistons, a polytetrafluoroethylene (PTFE) insulating body and fluorelastomer sealing rings, using a glass fibre membrane (Whatman glass microfiber filter) as the separator. The cells were assembled using the electrolytes listed in *Electrolyte characterization* subsection.

Electrochemical characterization. Electrochemical measurements of the EDLCs were performed at room temperature using a potentiostat/galvanostat (VMP3, Biologic) station controlled *via* its own software. Cyclic voltammetry (CV) measurements were performed at various voltage scan rates, from 5 mV/s to 1000 mV/s, after 10 preconditioning cycles at 100 mV/s. Once the CVs were completed, galvanostatic charge discharge (GCD) curves were recorded at specific currents ranging from 0.05 A/g to 50 A/g. The specific capacity (C_g) of the EDLCs (mAh/g) was calculated from the GCD curves as $C_g = (I \times t_d)/(3.6 \times m)$, where I is the applied current, t_d is the discharge time and m is the mass of the electrode materials. The gravimetric capacitance was calculated as gravimetric capacitance $= (I \times t_d)/(m \times \Delta V)$, where ΔV is the applied voltage window (*i.e.*, 1.4 V). The energy and power density were calculated using integral equations that consider the non-linearity of the GCD profiles, as discussed in refs.. [33,34]

Results

Figure 2a reports the ion conductivity of the investigated aqueous electrolytes as a function of the temperature. In general, amino acid-based electrolytes exhibit a conductivity lower than the one of reference electrolyte, *i.e.*, 2 M $NaNO_3$. For example, the ion conductivity of 2 M $NaNO_3$ is 100.1 mS/cm at room temperature (22 °C) (144.1 mS/cm at 80 °C), while 10 m Lys has a room temperature ion conductivity of 2.2 mS/cm (6.4 mS/cm at 80 °C). 10 m Pro + 2 M $NaNO_3$ exhibits intermediate ion conductivities, *i.e.*, 10.3 and 18.2 at room temperature and 80 °C. The trend of the ion conductivity trend is clearly correlated to that of the viscosities, which increase with the addition of the amino acid and decrease with the temperature (Figure 2b). The ion conductivity measured for 10 m Lys is consistent with the dielectric spectroscopy data presented in ref.[23] for the same solution at 23 °C. The imaginary part ε_r'' of the complex dielectric permittivity in the $10^4 - 10^6$ Hz frequency range allows the determination of the ionic conductivity *via* the relationship ionic conductivity $= 2\,\pi\,\varepsilon_r''\varepsilon_0 f$, where f is the frequency and ε_0 is the vacuum permittivity. An ionic conductivity of ~1.9 mS/cm, close to our experimental value of 2.2 mS/cm, is deduced from Figure S4 of ref.. [23] Regardless their lower conductivity compared to that of reference electrolyte, amino acid-based electrolytes still exhibit a modest ionic conductivity, on the same order of magnitude of prototypical organic electrolytes (*e.g.*, 1 M $TEABF_4$ in acetonitrile/propylene carbonate and ionic liquids established for EDLC applications). Prospectively, concentrations of amino acid lower than the one here studied (10 m) may be helpful to increase the overall ion conductivities of the electrolytes while retaining high ε_r, as here targeted for amino acid-based electrolytes (see discussion hereafter). The thermal properties of the amino acid-based electrolytes were studied through TGA and DSC measurements (Figure S1). More in detail, the TGA data measured for the L-lysine indicate a weight loss of ~6 wt% associated to water desorption, followed by amino acid degradation, starting from 130 °C and becoming significantly pronounced at temperatures above 180 °C (derivative of the weight loss > 0.4 %/C). L-proline exhibits negligible weight losses associated to water desorption, and its degradation starts at temperature higher than 200 °C. Overall, the thermal stability of these two amino acids does not restrict the operating temperature of EDLCs based on aqueous electrolytes, typically below the electrolyte boiling point. The boiling points of the amino acid-based electrolytes were estimated from onset temperatures of the first endothermic peaks occurring above 100 °C in their DSC curves (Fig-

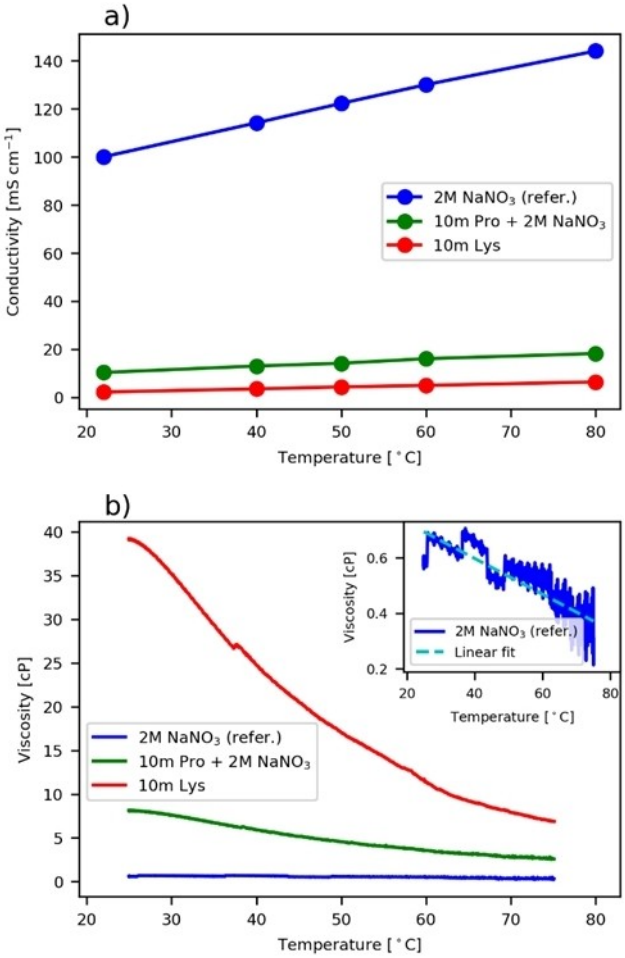

Figure 2. a) Ion conductivities of 10 m Lys (red), 10 m Pro + 2 M $NaNO_3$ (green) and reference 2 M $NaNO_3$ electrolyte (blue), measured as function of the temperature. b) Viscosities of 10 m Lys (red), 10 m Pro + 2 M $NaNO_3$ (green) and reference 2 M $NaNO_3$ electrolyte (blue), measured as function of the temperature. The inset panel show the enlargement of the viscosity data measured for 2 M $NaNO_3$, together with linear fit that indicates a linear correlation between the viscosity and the temperature.

Research Article
doi.org/10.1002/batt.202300458
Chemistry Europe
European Chemical Societies Publishing

ure S1). The estimated boiling points are 119 °C for 10 m Lys and 124 °C for 10 m Pro + 2 M $NaNO_3$. Noteworthy, the specimen evaporation in presence of purged gas causes a broadening of the endotherms, impeding an accurate boiling point determination. Thus, at the current stage, the boiling points values here given must be considered with precaution.

Figure 3a shows the CV curves acquired at voltage scan rates of 0.02 V/s, in a voltage window between 0 and 1.4 V, for the EDLCs based on the different electrolytes. The CV curves measured for the EDLCs at different voltage scan rates ranging from 0.01 to 1 V/s are reported in the Supplementary Information (Figure S2).

In this voltage window, the CV data show quasi-rectangular shapes supporting that L-lysine and L-proline are not redox-active amino acids on carbonaceous active materials. The only five proteogenic amino acids with known redox activity are cysteine, methionine, histidine, tryptophan and tyrosine,[35,36, 37] which, however, are not suitable for EDLCs applications due to their modest solubility and poor resistance against oxidation. At voltage above 1.3 V, Faradaic currents associated to whisker-like features in the CV curves may be associated to either irreversible water splitting reactions[38] or pseudocapacitive phenomena, like hydrogen electrosorption,[39,5] as previously shown in nearly neutral pH aqueous electrolytes. Despite their high concentration, amino acids are not widening ESW, which is typically widened with decreasing the water activity[5,6] because of the of increase the OER potential. This may indicate that Faradaic reactions are mainly associated with cathodic reactions, *e.g.*, hydrogen evolution reaction (HER) or hydrogen electrosorption. In accordance with previous literature[5,38,39] nanostructured carbons can strongly adsorb hydrogen in nearly neutral solutions, contrasting the completion of the HER through Heyrovsky and/or Tafel steps. Noteworthy, amino acids have solvation free energy in water similar to Na^+, Li^+ and NO_3^- ions, [40,41] which however are effective to widen the ESW of the electrolytes at high concentration (*e.g.*, 6 M for $LiNO_3$[5]). Also, differently from the ions of alkali metal nitrate salts, diffusivity of the amino acid molecules may be limited into microporous carbons, impeding efficient HER suppression.

Figure 3b shows the GCD curves for the investigated EDLCs based on different electrolytes, measured at specific current of 0.5 A/g. The discharge times for the EDCLs based on amino acid-containing electrolytes is higher than the one measured for the reference device without amino acids. The GCD curves recorded at different specific currents are shown in Supplementary Information (Figure S2).

Figure 4 shows the C_g and the corresponding gravimetric capacitance of the EDLCs as a function of the specific current, as calculated from the corresponding GCD curves. Importantly, at low specific currents $\leq$ 0.5 A/g, the EDLCs based on 10 m L-lysine electrolyte exhibited the highest C_g amongst the investigated devices, followed by the EDLCs based on 10 m L-proline + 2 M $NaNO_3$ electrolyte. At higher specific currents (*e.g.*, >2-3 A/g), the excessive viscosity of amino acid-based electrolytes (up to ~40 cP for 10 m Lys, Figure 2b)[42] limits the rate capability of the EDLCs. In addition, the size of amino acid molecules (~0.36-0.5 nm[43]) is larger than the nitrate salt ions (0.3-0.35[44]), which may instead easily access the micropores of the active materials, whose pore size distribution is shown in Figure S3.

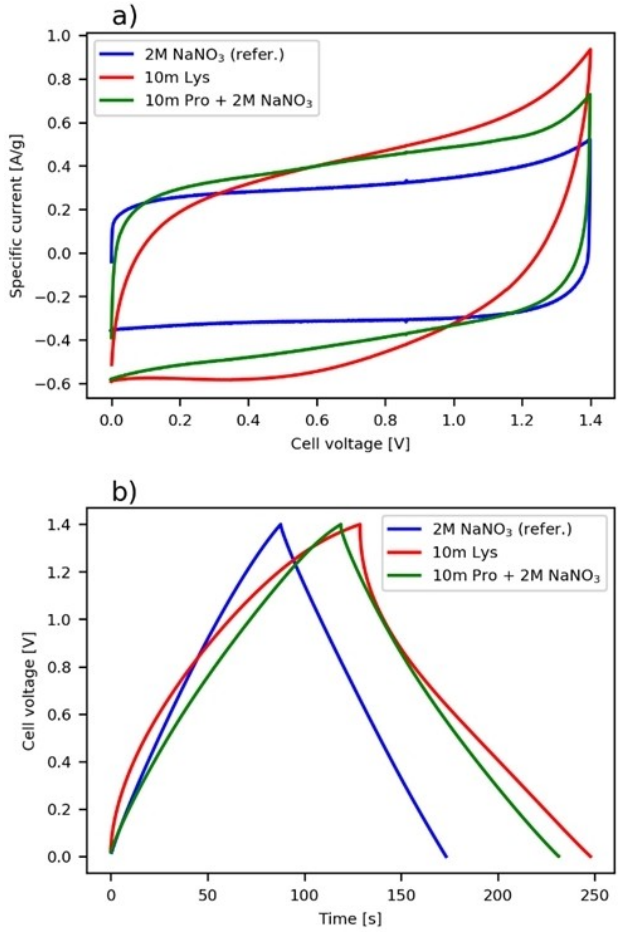

Figure 3. a) CV curves @0.02 V/s scan rate for 10 m Lys (red), 10 m Pro + 2 M $NaNO_3$ (green) and reference 2 M $NaNO_3$ electrolyte (blue). b) GCD curves @0.5 A/g for 10 m Lys (red), 10 m Pro + 2 M $NaNO_3$ (green) and reference 2 M $NaNO_3$ electrolyte (blue).

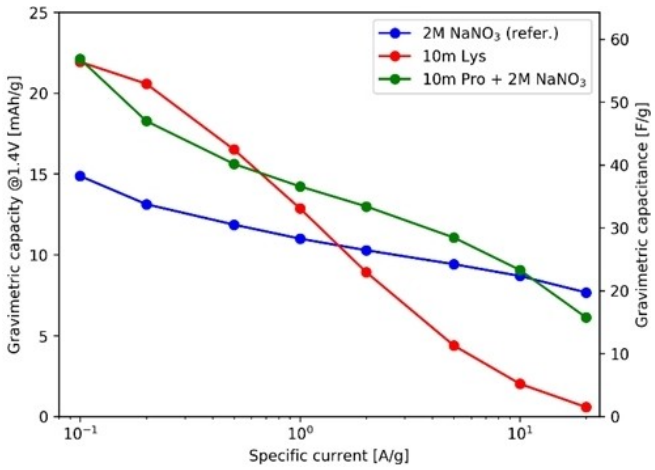

Figure 4. Gravimetric capacity @1.4 V (left y-axis) and the corresponding gravimetric capacitance (right y-axis) for 10 m Lys (red), 10 m Pro + 2 M $NaNO_3$ (green) and reference 2 M $NaNO_3$ (blue) electrolytes.

Research Article
doi.org/10.1002/batt.202300458
Chemistry Europe
European Chemical Societies Publishing

The non-straight shape of the GCD obtained with 10 m Lys is also a sign of ion diffusion limitations. Prospectively, the amino acid:salt weight ratio can be adjusted to determine an optimal trade-off between the ε_r and the viscosity of the electrolytes. Also, the porosity of the EDLC electrodes may be tailored based on the size of the amino acid molecules to enhance the ion accessibility to the electrode surface area. Alternatively, other biomolecules (amino acid derivatives) with still excellent dielectric properties but smaller size compared to the molecules here investigated, *e.g.*, γ-aminobutyric acid (GABA) or glycine, may be also evaluated.

Nevertheless, our overall CV and CGD data prove that, at low power density where the limited ion diffusion of amino acid-based electrolytes does not limit excessively the ion access to the electrode surface area, the formulation of electrolyte with high ε_r can significantly improve the C_g of aqueous EDLCs (by +50% at 0.1 A/g). Thus, the use of the amino acid additives in the electrolyte represents an effective strategy to improve the overall capacitive performance of aqueous EDLCs, as supported by the analytical model discussed in the next section.

To further validate the proposed amino acid-based electrolytes for practical applications, the cyclic stability of the corresponding EDLCs was assessed over 10000 GCD cycles (**Figure S4**). Except for the device based on the most viscous electrolyte, *i.e.*, 10 m Lys, the EDCLs showed satisfactory cyclic stability over 10000 GCD cycles at 5 A/g (capacity retention of 95.8 for 2 M $NaNO_3$ and 87.4% for 10 m Pro + 2 M $NaNO_3$). The performance fading observed for the EDCL based on 10 m Lys (capacity retention of 61.4% after 10000 GCD cycles) may be attributed to the solid precipitation that may occur upon prolonged cycling in presence of highly concentrated electrolytes (as in our case) and parasitic reactions, *e.g.*, water decomposition. Thus, the precipitate may clog the electrode porosity leading to a capacitance drop. The optimization of amino acid:salt weight ratio to tailor the viscosity of the amino acid-based electrolytes is promising strategy to increase the cyclic stability here presented for proof-of-concept devices.

Analytical model

An analytical model was used to estimate the enhancement of C_g, regulated by the incorporation of the amino acid additives, on an ideally flat highly oriented pyrolytic graphite (HOPG) slab.

The model accounts for the presence of both ions and zwitterionic amino acid molecules at the HOPG/electrolyte interface and for a Helmholtz layer with a limited maximum density of ions and zwitterions. Molecules cannot approach the electrode interface at zero distance due to their finite size. As discussed in the Supporting Information, the model is applied to EDLC operating at high voltage >0.4 V, where the effect of quantum capacitance caused by the finite density of electronic states of graphene sheets can be neglected. [9] In the Helmholtz layer, charges are supposed to lay at a minimum distance b from the interface, with a constant electric field and linear potential in the layer, as commonly modelled in the literature. [45] By assuming a constant electric field, the dielectric constant $\varepsilon_{HL}(E)$ is also uniform in the Helmholtz layer, since the displacement field, the product of $\varepsilon_{HL}(E)$ and electric field, is constant according to Gauss's law.

$\varepsilon_{HL}(E)$ in the Helmholtz layer depends on the local electric field in the layer (assumed constant) and is generally much inferior to that ε_r far away from the interface: the electric field and potential create a local concentration of charged ions close to the interface that reduces the dielectric constant of the electrolyte (competition between ions and dipoles). In the diffuse Gouy-Chapman layer, next to the Helmholtz layer, the electric field decays exponentially with the characteristic Debye length: since most of the voltage drop occurs in the Helmholtz layer, in the diffuse layer the ε_r is assumed to be independent on the (small) electric field and equal to the bulk value.

The continuity of the displacement field at the interface between Helmholtz layer and diffuse layer reads:

$$\varepsilon_{HL}(E)\ E = \varepsilon_r \frac{V_0 - E\ b}{\lambda_D}$$

where b is the thickness of the Helmholtz layer, V_0 is the electrode potential vs. the bulk solution, $\lambda_D = \sqrt{\frac{\varepsilon_0 \varepsilon_r\ KT}{2\ c\ N_A e^2}}$ is the Debye length (depending on the ion molarity c), $\frac{V_0 - E\ b}{\lambda_D}$ is the electric field of the diffuse layer at the interface with the Helmholtz layer, ε_{HL} the dielectric constant of the Helmholtz layer and E is the electric field in the Helmholtz layer. The above expression is solved as an implicit equation to derive the unknown electric field E in the Helmholtz layer, from which the dielectric permittivity $\varepsilon_{HL}(E)$ in the Helmholtz layer and the Stern specific capacitance per unit surface $C_{HL} = \varepsilon_0 \varepsilon_{HL}(E)/b$ can be extrapolated. For our case, the specific capacitance of the diffuse Gouy-Chapman layer, $C_{diff} = \frac{\varepsilon_0 \varepsilon_r}{\lambda_D} \cosh\left(\frac{zFV}{2RT}\right) \approx \varepsilon_0 \varepsilon_r / \lambda_D$, is much higher than the C_{HL}, and can be therefore neglected since the two capacitance are in series.

The analytical expression of $\varepsilon_{HL}(E)$ is given by the Iglic-Gongadze model, [18,46] as summarized in the Supplementary Information. Briefly, the bulk ε_r of 2 M $NaNO_3$ aqueous solution is assumed to be 58 according to the Molecular Dynamics (MD) and dielectric spectroscopy data, [49,50] while for 10 m (c_{H2O} ≈40%w) L-lysine solution, ε_r was assumed to be 300, as derived from bulk dielectric spectroscopy at 296 K. [23] Finally for L-proline, experimental data at our 10 m concentration is not available, so that an indicative value of $\varepsilon_r = 180$ were used for 10 m Pro + 2 M $NaNO_3$. This value can be considered as a conservative estimate from the experimental ε_r measured for 5.569 M L-proline (*i.e.*,182). [47] In [47], it is shown that 2 M NaCl reduce the bulk $\varepsilon_r$of 0.6 M L-proline by *ca.* 20%; the expected dielectric reduction of 2 M $NaNO_3$ after adding 10 m L-proline should be less, since the relative weight of the zwitterionic content in the electrolyte is much greater. The thickness of the Helmholtz layer is not known with precision, but we performed a sensitive analysis on a reasonable range based on neutron diffraction data[48] and MD-simulated radial pair distribution function g(r). [49,51] The position of the first peak in the g(r) is an indication for the thickness of the monomolecular Helmholtz

layer at the electrode/electrolyte interface. In [44], the hydrated ionic radius is rated 3.58 Å for Na^+ and 3.35 Å for NO_3^-, while the radii for L-proline and L-lysine the respective radii are 3.61 Å and 5.02 Å, respectively, based on the analysis of contacting residues in existing proteins. [43] A range of 2.5-3.5 Å is assumed for the Helmholtz layer of pure 2 M $NaNO_3$ electrolyte while a slightly higher range 3–5 Å is expected in the presence of 10 m L-proline due to the larger size of the amino acid molecule; lastly, a conservative range 6–8 Å is assumed for 10 m L-lysine, since in this case the ion size of charged L-lysine$^+$ and L-lysine$^-$ is bigger than Na^+ and NO_3^-.

In the simplified framework of the above model, it is possible to show that amino acid addition to the water:salt electrolyte dramatically improves the $\varepsilon_r$of the electrolyte, increasing the surface capacitance of the HOPG/electrolyte interface (Figure 5). The mild dependence of the surface capacitance on the Helmholtz layer thickness b indicates the robustness of the model.

The expected surface capacitance enhancement for a flat HOPG/electrolyte interface after the addition of amino acids, from ~5-fold at high voltage up to ~10-fold at low voltages, is even greater than those experimentally observed using electrode based on nanoporous activated carbon and graphene. We speculate that ion diffusion limitations can currently limit the enhancement of actual capacitance of our EDLCs, even though the optimization of the electrode morphology and electrolyte formulation may unlock the EDLC performance towards the theoretical one. As voltage increases, Na^+ and NO_3^- ions overcome amino acid zwitterions at the electrode interface and the specific capacitance drops. For the reference case with no amino acids, the takeover of salt ions on the water dipoles already occurs at a low voltage. Thus, for voltage $>$0.6 V, the surface capacitance reaches an asymptotic value of ~6 μF/cm^2), while in the presence of amino acids, the asymptotic value is estimated at voltage $>$1.4 V. The asymptotic value of for the specific capacitance of the reference electrolyte is in line with values reported in the literature for graphene multilayers. [9] The performance of 10 m Lys and 10 m Pro + 2 M $NaNO_3$ derived by the model are similar, as confirmed by our experimental investigation (Figures 3 and Figures 4) in a condition (slow ramps, low current) where the larger size L-lysine molecule compared to that pf L-proline has not a penalizing effect on amino acid accessibility to micropores of the active materials.

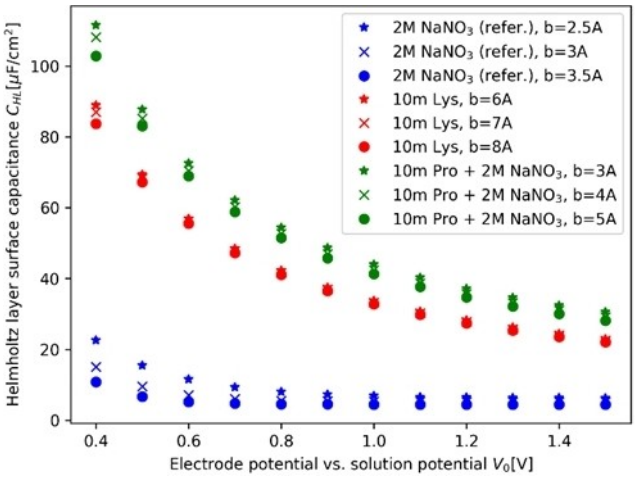

Figure 5. Calculated Stern (Helmholtz layer) surface capacitance for the amino acid-based electrolytes (10 m L-lysine and 10 m L-proline + 2 M $NaNO_3$) compared to the surface capacitance for the reference electrolyte (2 M $NaNO_3$, in blue), plotted for different thickness of the Helmholtz layers.

Conclusions

We experimentally tested a new concept of EDLCs based on sustainable aqueous electrolytes with a large concentration (10 m) of dissolved amino acids and a modest concentration (2 M) of $NaNO_3$ salts. The former increases the ε_r of the electrolyte, while the latter increase the electrolyte ionic conductivity. The performance of CV curves and GCD curves analysis highlighted a +50% increased capacitance at the low specific currents of 0.1 A/g compared to the reference electrolyte with 2 M $NaNO_3$ and no amino acids. Importantly, our analytical model predicts even a greater (5-10-fold) capacitance enhancement compared to experimental values, likely due to actual performance limit associated with a difficult access of amino acids to the active material micropores, whose average size (~9 Å) is comparable to that of the amino acid.

As future developments, the active material porosity could be optimized to offer a tradeoff between a lower specific surface area and a much easier access to the carbon nanopores, leading to optimal specific capacity/surface capacitance and rate capability, as well as enhanced ESW. Furthermore, salt concentration could be increased at least for L-proline-based electrolyte, without affecting the transport properties measured for 10 m amino acid concentration and 2 M salt.

It would be also interesting to extend this concept of zwitterionic electrolytes using other types of high-ε_r amino acid derivatives sharing the requirements of sustainability (both environmental and economic), large dipolar moment, excellent solubility in water, modest molecule size, operation at pH close to neutral, which, in turn, hampers side reactions in extended voltage windows. Excellent candidates are GABA, taurine and carnitine, which are cheap and widely available dietary supplements with a huge ε_r. [52] These amino acid derivatives with no side chain are expected to fit better in the micropores of advanced active materials, improving diffusion process of the amino acid investigated herein. As a secondary choice, glycine and trimethyl glycine betaine still have large $\varepsilon_r$and satisfactory solubility in water and are smaller than L-lysine and L-proline. Trimethylamine N-oxide (TMAO) is also a dipolar zwitterionic natural compound used by fish, mollusks and crustaceans as a contrasting agent to the protein-destabilizing action of salt and pressure, although its cost is sensibly higher than the amino acid derivatives above.

We believe that the design of the next-generation EDLCs could take inspiration from nature and be enabled by low-cost, green and widely available materials, such as water, carbon, amino acid biomolecules and common inorganic salts.

Acknowledgements

Part of this project received funding from the European Union's Horizon 2020 research and innovation program under Grant Agreement No. 881603-GrapheneCore3, the European Union's SENSIBAT project under Grant Agreement No. 957273, the European Union's GREENCAP Horizon Europe research and innovation program under Grant Agreement No. 101091572.

Conflict of Interests

The authors of this manuscript belong to a company, Ansaldo Green Tech S.p.A or BeDimensional S.p.A.

Data Availability Statement

The data that support the findings of this study are available from the corresponding author upon reasonable request.

Keywords: supercapacitor · amino acid · sustainable · electrolyte · dielectric permittivity

[1] P. Sharma, T. S. Bhatti, *Energy Convers. Manage.* **2010**, *51 12*, 2901–2912.
[2] A. Krause, A. Balducci, *Electrochem. Commun.* **2011**, *13 8*, 814–817.
[3] M. A. Garakani, S. Bellani, V. Pellegrini, R. Oropesa-Nunez, A. E. Del Rio Castillo, S. Abouali, L. Najafi, B. Martin-Garcia, A. Ansaldo, P. Bondavalli, C. Demirci, V. Romano, E. Mantero, L. Marasco, M. Prato, G. Bracciale, F. Bonaccorso, *Energy Storage Mater.* **2021**, *34*, 1–11.
[4] J. Zhao, A. F. Burke, *Adv. Energy Mater.* **2021**, *11 1*, 2002192.
[5] M. Eredia, S. Bellani, M. I. Zappia, L. Gabatel, V. Galli, A. Bagheri, H. Beydaghi, G. Bianca, I. Conticello, V. Pellegrini, F. Bonaccorso, *APL Mater.* **2022**, *10*, 101102.
[6] T. Liang, R. Hou, Q. Dou, H. Zhang, X. Yan, *Adv. Funct. Mater.* **2021**, *31 3*, 2006749.
[7] D. R. Joshi, A. Nisha, *J. Pharm. Res. Int.* **2019**, *28 3*, 2456–9119.
[8] A. Burke, *Eletrochim. Acta.* **2007**, *53 3*, 1083–1091.
[9] H. Ji, X. Zhao, Z. Qiao, J. Jung, Y. Zhu, Y. Lu, L. L. Zhang, A. H.Mac Donald, R. S. Ruoff, *Nat. Commun.* **2014**, *5 3317*.
[10] T. R. Griffiths, D. C. Pugh, *Coord. Chem. Rev.* **1979**, *2 3*, 129–211.
[11] S. Dong, W. Gao, K. Shi, Q. kang, Z. Xu, J. Yuan, Y. Zhu, H. Li, J. Chen, P. Jiang, G. Wu, Q. Wei, J. Qiu, X. Qian, X. Huang, *Cell Rep. Phys. Sci.* **2023**, *4 2*, 101284.
[12] R. Biczak, *J. Hazard. Mater.* **2016**, *304 5*, 173–185.
[13] K. Egorova, V. Ananikov, *ChemSusChem* **2014**, *7 2*, 336–360.
[14] C. Schuetter, S. Pohlmann, A. Balducci, *Adv. Energy Mater.* **2019**, *9 25*, 190334.
[15] N. Blonquist, T. Wells, B. Andres, J. Backstrom, S. Forsberg, H. Olin, *Sci. Rep.* **2017**, *7*, 39836.
[16] J. Han, A. Mariani, S. Passerini, A. Varzi, *Energy Environ. Sci.* **2023**, *16*, 1480–1501.
[17] S. Millefiori, A. Alparone, A. Millefiori, A. Vanella, *Biophys. Chem.* **2008**, *132 2–3*, 139–147.
[18] E. Gongadze, A. Iglic, *Bioelectrochemistry* **2012**, *87*, 199–203.
[19] S. Sarkar, A. Guha, T. N. Narayanan, J. Mondal, *chemrXiv preprint* **2022**, DOI: 10.26434/chemrxiv-2022-ttm2 s.
[20] S. Knapp, R. Ladenstein, E. A. Galinski, *Extremophiles* **1999**, *Aug 3 3*, 191–8.
[21] C. F. Baxter, C. L. Ortiz, *Life Sci.* **1966**, *5 24*, 2321–2329.
[22] J. C. Measures, *Nature* **1975**, *257*, 398–400.
[23] S. Cerveny, J. Swenson, *Phys. Chem. Chem. Phys.* **2014**, *16*, 22382–22390.
[24] N. A. Bowden, J. P. M. Sanders, M. E. Bruins, *J. Chem. Eng. Data* **2018**, *63 3*, 488–497.
[25] J. Qiu, H. Huang, H. He, H. Liu, S. Hu, J. han, D. Yi, M. An, P. Wang, *J. Chem. Eng. Data.* **2019**, *64 12*, 5920–5928.
[26] M. Aliyeva, P. Brandao, J. R. B. Gomes, J. A. P. Coutinho, O. Ferreira, S. P. Pinho, *Ind. Eng. Chem. Res.* **2022**, *61 16*, 5620–5631.
[27] S. Bellani, B. Martin-Garcia, R. Oropesa-Nunez, V. Romano, L. Najafi, C. Demirci, A. E. Del Rio Castillo, L. Marasco, E. Mantero, G. D'angelo, F. Bonaccorso, *Nanoscale Horiz.* **2019**, *4*, 1077–1091.
[28] A. E. Del Rio Castillo, V. Pellegrini, A. Ansaldo, F. Ricciardella, H. Sun, L. Marasco, J. Buha, Z. Dang, L. Gagliani, E. Lago, N. Curreli, S. Gentiluomo, F. Palazon, M. Prato, R. Oropesa-Nunez, P. S. Toth, E. Mantero, M. Crugliano, A. Gamucci, A. Tomadin, M. Polini, F. Bonaccorso, *Mater. Horiz.* **2018**, *5*, 890–904.
[29] S. Bellani, E. Petroni, A. E. Del Rio Castillo, N. Curreli, B. Martin-Garcia, R. Oropesa-Nunez, M. Prato, F. Bonaccorso, *Adv. Funct. Mater.* **2019**, *29 14*, 1807659.
[30] M. I. Zappia, V. Mastrodonardi, S. Bellani, Y. Zuo, G. Bianca, L. Gabatel, M. Gentile, A. Bagheri, H. Beydaghi, F. Drago, M. Ferri, M. Moglianetti, P. P. Pompa, L. Manna, F. Bonaccorso, *Electrochim. Acta* **2023**, *462*, 142696.
[31] A. Bagheri, S. Bellani, H. Beydaghi, M. Eredia, L. Nayafi, G. Bianca, M. I. Zappia, M. Safarpour, M. Najafi, E. Mantero, Z. Sofer, G. Hou, V. Pellegrini, X. Feng, F. Bonaccorso, *ACS Nano* **2022**, *16 10*, 16426–16442.
[32] M.Najafi, S.Bellani, V.Galli, M.I:Zappia, A.Bagheri, M.Safarpour, H.Beydaghi, M.Eredia, L.Pasquale, R.Carzino, S.Lauciello, J. K.Panda, R.Brescia, L.Gabatel, V.Pellegrini, F.Bonaccorso, *Electrochemistry* **2022**, *3*, 463–478.
[33] A. Laheaar, P. Przygocki, Q. Abbas, F. Beguin, *Electrochem. Commun.* **2015**, *60*, 21–25.
[34] A. Noori, M. F. El-Khady, M. S. Rahmanifar, R. B. Kaner, M. F. Mousavi, *Chem. Soc. Rev.* **2019**, *48*, 1272.
[35] A. H. B. Dourado, F. C. Pastrian, S. I. Cordoba de Torresi, *An. Acad. Bras. Cienc.* **2018**, *90(1)*, 607–630.
[36] V. Brabec, V. Mornstein, *Biophys. Chem.* **1980**, *12 2*, 159–65.
[37] M. E. Weese-Myers, A. E. Ross, *J. Electrochem. Soc.* **2021**, *168*, 126524.
[38] Q. Abbas, B. Gollas, V. Presser, *Energy Technol.* **2019**, *7 9*, 1900430.
[39] S. E. Chun, J. F. Whitacre, *J. Power Sources* **2013**, *242*, 137–140.
[40] Y. Markus, *J. Chem. Soc. Faraday Trans.* **1987**, *83*, 2985–2996.
[41] S. B. Dixit, R. Bhasin, E. Rajasekaran, B. Jayaram, *J. Chem. Soc. Faraday Trans.* **1997**, *93 6*, 1105–1113.
[42] M. Eudaimon, *CHIEAM Options Méditerranéennes (Zaragoza)* **1999**, 295–301 https://om.ciheam.org/om/pdf/c37/99600029.pdf.
[43] S. Liu, X. Xiang, H. Liu, *biorXiv preprint* **2022**, DOI: 10.1101/463554.
[44] C. Zhong, D. Yida, J. Qiao, *Chem. Soc. Rev.* **2015**, *44 21*, 7431–7920.
[45] A. Velikonja, E. Gongadze, V. Kralj-Iglic, A. Iglic, *Int. J. Electrochem. Sci.* **2014**, *9*, 5885–5894.
[46] A. Iglic, E. Gongadze, *J. Phys. Conf. Ser.* **2012**, *398*, 012004.
[47] O. A. Dmitrieva, M. V. Fedotova, R. Buchner, *Phys. Chem. Chem. Phys.* **2017**, *19*, 20474.
[48] S. E. McLain, A. K. Soper, A. E. Terry, A. Watts, *J. Phys. Chem. B* **2007**, *111 17*, 4568–4580.
[49] H. Krienke, *Condens. Matter Phys.* **2013**, *16*, 1–12.
[50] J. Mollerup, M. P. Breil . *AIChE J.* **2015**, *61 9*, 2854–2860.
[51] S. Dasetti, J. K. Barrows, S. Sarupria, *Soft Matter* **2019**, *15 11*, 2359–2372.
[52] J. Hou, S. M. Abie, R. Strand-Amundsen, Y. Galperin, J. Bergli, C. Schuelke, S. H. Zadeh, O. G. Martinsen, *Sci. Rep.* **2021**, *11*, 18082.
[53] L. Onsager, *J. Am. Chem. Soc.* **1936**, *58*, 1486.
[54] P. Debye, E. Huckel, *Phys. Z.* **1923**, *24*, 185–206.
[55] Q.Tang, *"Theory of the dielectric constant of polar liquids"*, Master Thesis, The Pennsylvania State University, **2014**.
[56] A. J. Pak, E. Paek, G. Hwang, *Phys. Chem. Chem. Phys.* **2013**, *15*, 19741.
[57] C. Zhan, J. Neal, J. Wu, D. Jiang, *J. Phys Chem. C* **2015**, *119*, 22297–22303.
[58] K. A.Dill, S.Bronberg, *"Molecular Driving Forces: Statistical Thermodynamics in Biology, Chemistry, Physics and nanoscience, 2ed."*, **2011**, ISBN 978–0-8153-4430-8.

Manuscript received: October 8, 2023
Revised manuscript received: December 13, 2023
Accepted manuscript online: December 24, 2023
Version of record online: January 17, 2024